Complex-ω approach versus complex-k approach in description of gain-assisted surface plasmon-polariton propagation along linear chains of metallic nanospheres

Indika B. Udagedara, Ivan D. Rukhlenko,* and Malin Premaratne
Advanced Computing and Simulation Laboratory (AχL), Department of Electrical and Computer Systems Engineering, Monash University, Clayton, VIC 3800, Australia

(Received 4 December 2010; revised manuscript received 9 February 2011; published 28 March 2011)

Propagation characteristics of surface plasmon-polaritons (SPPs) in linear chains of metallic nanospheres (LCMNs) can be found from a dispersion equation, by assuming that either frequency or wave number of a SPP is real. In this paper, we present a comparative study of SPP modes corresponding to the two types of complex solutions for an infinitely long LCMN embedded in a gain medium. We show that even though gain predominantly affects the SPP dispersion obtained with real frequency, both solutions result in the same dispersion and attenuation of SPP modes, when Ohmic losses are almost compensated by gain. In this regime, an analytic expression for the propagation length of SPPs exists, and the SPPs' dispersion is determined by a real equation. We also demonstrate that for a given amount of gain (below the amplification limit of $\sim$1000 cm^{-1}), transversely polarized SPPs attenuate slower than longitudinally polarized SPPs and are, therefore, preferable for the purpose of energy transfer in gain-supplied LCMNs. The transmission windows for SPP modes of different polarizations do not overlap each other, which facilitates realization of LCMN-based plasmonic filters. Our results may prove useful in design optimization of all-optical chips for power-efficient optical supercomputers.

DOI: 10.1103/PhysRevB.83.115451 PACS number(s): 73.20.Mf, 42.79.Gn, 42.70.Hj, 81.05.Xj

I. INTRODUCTION

Optical excitation of metal-dielectric interfaces induce oscillations of free-electron plasma coupled to an electromagnetic field, which are known as surface plasmon-polaritons (SPPs).[1–3] Owing to the strong spatial localization of SPPs near the interfaces, they can be used to transfer optical signals in a nanoscale photonic circuitry.[4–6] Several types of metal-dielectric nanostructures, such as chains of periodically arranged nanoparticles,[7] nanowires[8] and nanostrips,[9] thin films,[10] and sharp wedges[11] have been proposed for this purpose. Unfortunately, the employment of these nanostructures forces a compromise between the confinement and dissipation of the guided SPP modes they support. For example, metallic films and nanostrips enable propagation of SPPs over hundreds of micrometers at the expense of poor confinement.[2] In contrast, chains of metallic nanospheres offer deep subwavelength localization of SPPs but cause them to fully decay on the length scale of only a few micrometers.[12] To increase the propagation length of SPPs in chains of metallic nanoparticles, a plethora of theoretical and experimental studies have been conducted during the last decade.[12–24]

Although the evolution of SPP modes in a metal-dielectric nanostructure can, in principle, be analyzed with the standard finite-element method or finite-difference time-domain (FDTD) technique,[25] the fine grid, required to adequately capture all geometrical features of the nanostructure, makes these methods computationally inefficient.[26,27] For instance, to simulate the propagation of a 1-fs SPP pulse along a 0.5-μm-long chain of seven metallic nanospheres with radii of 25 nm (using a $160 \times 40 \times 40$ FDTD grid), it takes about 16 hours of a 4-CPU 3.17-GHz computer time. The analysis of SPP evolution can actually be performed much faster, due to the fact that the characteristic dimensions of nanoparticles ($\sim$100 nm) are much smaller than the SPP's wavelength, which varies from several micrometers to 600 nm for the spectral range from 0.4 to 2 μm.[28,29] A substantial simplification in the description of plasmonic nanostructures is achieved by treating metallic nanoparticles as point dipoles and considering SPPs as waves in the system of coupled dipoles. [7,20,21,24]

According to the classical electrodynamics, the electric field generated by a radiating dipole decays with distance r as $\propto 1/r^3$ in the near zone, $\propto 1/r^2$ in the intermediate zone, and $\propto 1/r$ in the far zone.[30,31] In the initial works, it was assumed that the energy transport through linear chains of metallic nanospheres (LCMNs) is predominantly caused by the near field.[24,27] However, as later studies revealed, taking into account the fields from all three zones is required for the proper description of SPP propagation.[21] The basic characteristics of SPP modes are determined by the dispersion equation, whose solution specifies either a complex wave number as a function of real frequency (complex-k solution), or a complex frequency as a function of real wave number (complex-ω solution).[32] Even though these two types of solutions have never been analyzed simultaneously in the available literature, their brief comparison based on the results independently obtained by several research groups shows that they are rather different.[13,17,20,21] In this paper, we compare the complex-k and complex-ω solutions in detail, and demonstrate that their difference is caused by the strong dissipation of SPP modes; both solutions lead to the same propagation characteristics when loss is compensated by gain.

Supplying metal-dielectric nanostructures with gain began to be considered not long ago, once their practical applications became a reality.[33,34] It was shown that the damping of the surface plasmon resonance associated with a metal nanoparticle can be suppressed by embedding the nanoparticle in an optically active medium.[35,36] This phenomena was experimentally observed by Noginov *et al.*,[37] who later employed it to create a tiny laser using gold nanospheres coated with dye-doped silica.[38] It was also demonstrated, with the approximate complex-ω solution, that SPPs can be amplified

if the host dielectric provides a sufficiently large gain.[20,39] Since the above works do not focus on the applicability of the complex-ω and complex-k solutions for description of gain-assisted SPP propagation along LCMNs, such an analysis is still in demand.

In this paper, we thoroughly compare the characteristics of SPP modes obtained with complex-ω and complex-k solutions, for LCMN-based plasmonic waveguides in the presence of gain. We start our analysis in Sec. II, by briefly discussing the modifications that should be made to the coupled dipole equations, to allow for gain in infinite-length LCMNs. In Sec. III, we describe the main features of longitudinal and transverse SPP modes in the absence of gain. The effect of gain on SPPs is investigated in Sec. IV. We show there that gain has a different impact on SPP modes obtained with different types of complex solutions, and also present a simplified version of the dispersion equation for the case where loss is nearly compensated by gain. Finally, in Sec. V, we validate our conclusions for the complex-k solution by simulating propagation of the ultrashort SPP pulse along a finite-length LCMN. We summarize our result and conclude the paper in Sec. VI.

II. THEORY OF SPP DISPERSION IN THE PRESENCE OF GAIN

The dispersion of SPPs in a finite, linear chain of metallic nanospheres (LCMNs) consists of normal modes, whose number depends on the total number of nanospheres, N. When the nanospheres are treated as point dipoles, the frequencies of the normal modes (normal frequencies) make the determinant of the $2N \times 2N$ matrix that describes electromagnetic coupling between the dipoles vanish. Since no general analytic expression exists for the secular equation in this case, the problem of calculating normal frequencies becomes increasingly time consuming, as the chain grows in length. Fortunately, the optical properties of LCMNs with $N \gtrsim 10$ do not differ much from those for infinite-length LCMNs,[26] which allows us to study the dispersion of SPPs in relatively long chains by assuming N to be infinite.

With the above fact in mind, consider an infinite LCMN embedded in an unbounded active medium of permittivity $\varepsilon_h = n_h^2$, where $n_h = n_h' + in_h''$ is the complex refractive index with a negative imaginary part (from here onward, we mark the real and imaginary parts of a complex number by one and two primes, respectively). Let nanospheres of radii R be spaced at a intervals. In the dipole approximation, which is justified for the description of an LCMN as long as $a/R \geqslant 3$,[21,22] the electric dipole moment $\tilde{\mathbf{p}}_n$, induced on the nth nanosphere, is related to the local electric field $\tilde{\mathbf{E}}_n$ through polarizability α via $\tilde{\mathbf{p}}_n = \alpha\tilde{\mathbf{E}}_n$ (hereafter, we use a tilde to denote Fourier transform of a time-domain function in the frequency domain). The polarizability of a nanosphere depends on its internal structure and the optical properties of the surrounding medium. For a homogeneous nanosphere of permittivity ε_m, it is found from the relation[17,40,41]

$$\frac{1}{\alpha} = \frac{1}{\alpha_0} - \frac{2}{3}\frac{iq^3}{\varepsilon_h},$$

where $\alpha_0 = \varepsilon_h(\varepsilon_m - \varepsilon_h)/(\varepsilon_m + 2\varepsilon_h)R^3$ is the quasistatic polarizability, $q = n_h\omega/c$, and c is the speed of light in a vacuum; the last term in this expression accounts for the radiative decay of SPPs. If the nanosphere has one or several dielectric cores, the expression for α_0 is more involved.[31,42]

The electric field acting on the nth nanosphere is the sum of the fields generated by all other nanospheres and external sources,[21] i.e.,

$$\tilde{\mathbf{E}}_n = \frac{1}{\varepsilon_h}\sum_{j\neq n}\left[(1 - iq|n-j|a)\,\frac{3\,(\tilde{\mathbf{p}}_j\cdot\mathbf{e}_L)\,\mathbf{e}_L - \tilde{\mathbf{p}}_j}{(|n-j|a)^3} + q^2\,\frac{\tilde{\mathbf{p}}_j - (\tilde{\mathbf{p}}_j\cdot\mathbf{e}_L)\,\mathbf{e}_L}{|n-j|a}\right]\exp(iq|n-j|a) + \tilde{\mathbf{E}}_n^{(\mathrm{ext})}, \quad (1)$$

where $\mathbf{e}_L$ is the unit vector in the propagation direction, and an optical disturbance is assumed to vary in time as $\propto \exp(-i\omega t)$.

The dispersion of SPPs can be derived from the identity

$$\tilde{\mathbf{p}}_n = \alpha\tilde{\mathbf{E}}_n \quad (2)$$

in the absence of the external sources. By decomposing the electric field into transverse and longitudinal components, $\tilde{\mathbf{E}}_n \equiv (\tilde{\mathbf{E}}_n\cdot\mathbf{e}_L)\,\mathbf{e}_L + \mathbf{e}_L\times[\tilde{\mathbf{E}}_n\times\mathbf{e}_L]$, and setting $\tilde{\mathbf{p}}_n = \tilde{\mathbf{p}}_0\exp(ikna)$ in Eq. (1), we obtain from Eq. (2) the dispersion relation

$$\Phi_3 - iqa\Phi_2 = \varepsilon_h a^3/(2\alpha) \quad (3)$$

for the longitudinally polarized SPPs, and

$$\Phi_3 - iqa\Phi_2 - (qa)^2\Phi_1 = -\varepsilon_h a^3/\alpha \quad (4)$$

for the transversely polarized SPPs. Here, the function Φ_j $(j = 1,2,3)$ is defined as

$$\Phi_j = \mathrm{Li}_j\{\exp[i(q+k)\,a]\} + \mathrm{Li}_j\{\exp[i(q-k)\,a]\},$$

where $\mathrm{Li}_j(z)$ is the common polylogarithm.[43]

The complex roots (ω,k) of Eqs. (3) and (4) determine the dependance of the SPPs' frequency on the wave number k. In the quasistatic limit and in the absence of Ohmic losses, these equations yield the dispersion law of the analytic form $\omega(k)$.[21] In the realistic situation, an approximate solution for Eqs. (3) and (4) can be obtained by perturbatively evaluating their left-hand sides near the surface-plasmon resonance frequency of a single nanosphere.[20,39] For frequencies far from the resonance, such a solution becomes inaccurate, and the the roots (ω,k) need to be calculated numerically.

It should be noted that when the decay of SPPs dominates their amplification resulting from gain, the function Φ_j diverges in the lower half-plane of complex ω for real k [due to the factors $\exp(iqa)$], and also in the upper half-plane of complex k for real ω [due to the factor $\exp(-ika)$]. In the former case, an analytic continuation of both polylogarithms in Φ_j is required from the region $\omega'' < 0$, while in the latter case, only the second polylogarithm should be analytically continued, because $k'' > 0$. The situation is different when a net amplification of SPPs occurs along an LCMN. In this instance, $\omega'' > 0$ for real k, and $k'' < 0$ for real ω, so that analytic continuation from the upper half-plane, $k'' > 0$, is required only for the first polylogarithm in Φ_j.[44] With such modifications, Eqs. (3) and (4) can be evaluated in all situations of practical interest.

The results presented in the following sections are obtained by numerically solving Eqs. (3) and (4) with Wolfram Mathematica 7. In order to facilitate the complex-root search procedure, we use approximate analytical solutions to the dispersion equations as initial guesses for the root-finding algorithm. The analytical solutions are derived by considering the electrostatic limit ($q \to 0$) and allowing for only the nearest-neighbor interaction between the nanospheres. These approximations yield $\Phi_j = 2\cos(ka)$, so that Eqs. (3) and (4) reduce to the relations

$$k(\omega) = (1/a)\cos^{-1}[\varepsilon_h a^3/(4\alpha)]$$

and

$$k(\omega) = (1/a)\cos^{-1}[-\varepsilon_h a^3/(2\alpha)].$$

In Sec. V, the propagation of SPP pulse is modeled using MATLAB 7.8.

III. DISPERSION OF SPP MODES IN THE ABSENCE OF GAIN

The roots of Eqs. (3) and (4) are generally given by pairs of complex numbers $(\omega' + i\omega'', k' + ik'')$. Physically, only those of the pairs that have either real frequency or real wave number are interesting. In what follows, we refer to the first type of roots, $(\omega_1', k_1' + ik_1'')$, as the complex-$k$ solution, whereas the second type of roots, $(\omega_2' + i\omega_2'', k_2')$, is referred to as the complex-ω solution. A complex-k solution describes the situation in which SPP mode decays spatially along an LCMN, but the magnitudes of the nanospheres' polarizations do not change in time. On the other hand, a complex-ω solution corresponds to the dissipation of SPPs inside a resonator, when the polarizations of all nanospheres decay in time rather than in space. Obviously, different experimental techniques are required to verify theoretical predictions for these two scenarios.[13]

In Figs. 1(a) and 1(b), we plot typical SPP dispersion in an LCMN for the complex-k and complex-ω solutions of Eqs. (3) and (4), in the absence of gain. We assume that the chain is made of silver nanospheres embedded in silica glass ($n_h = 1.5$) and use the following parameters: $R = 25$ nm, $a = 75$ nm, $\varepsilon_m = \varepsilon_\infty - \omega_p^2/(\omega^2 + i\gamma\omega)$, $\varepsilon_\infty = 5$, $\omega_p = 9.5$ eV, and $\gamma = 0.1$ eV.[45] For versatility of our plots and conclusions, the frequencies and wave numbers are expressed in the natural units of $2\pi c/a$ and $2\pi/a$. As usual, the dispersion branches above the light line (dashed) correspond to the radiative SPPs, and the branches below the light line represent guided SPPs that do not easily interact with light due to the wave vector mismatch.[46,47] It is seen from Fig. 1(a) that the dispersion of the longitudinally (L) polarized SPP mode differs noticeably for the cases of complex-k and complex-ω solutions. The two dispersion branches overlap only in the vicinity of the surface-plasmon frequency,[48] $\omega_{SP} = \omega_p/(\varepsilon_\infty + 2\varepsilon_h')^{1/2} \approx 0.186$, where they intersect the light line, but dramatically deviate from each other elsewhere. Specifically, near the Brillouin zone edge, the complex-k curve

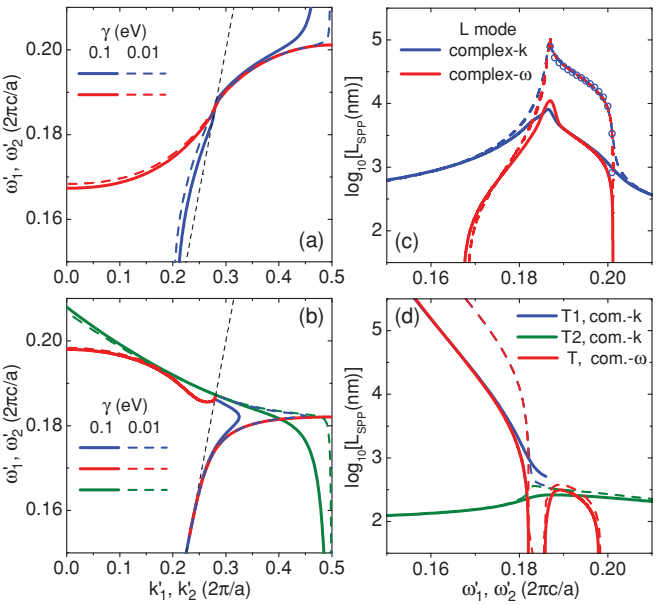

FIG. 1. (Color online) Dispersion of (a) longitudinally (L) and (b) transversely (T, T_1, T_2) polarized SPP modes for complex-k and complex-ω solutions of Eqs. (3) and (4), in the absence of gain; panels (c) and (d) show the corresponding propagation lengths; dashed is the light line for host medium. For comparison, dashed curves represent a hypothetic low-loss material with $\gamma = 0.01$ eV. For simulation parameters refer to text.

bends upward, while the complex-ω solution approaches the frequency

$$\omega_{2L}' \approx \frac{\omega_p}{\sqrt{\varepsilon_\infty - \chi_L \varepsilon_h'}} \approx 0.2, \tag{5}$$

with $\chi_L = [3\zeta(3) - 2(a/R)^3]/[3\zeta(3) + (a/R)^3]$ and $\zeta(3) \approx 1.202$ being the Riemann zeta function.[49] In obtaining this frequency from Eq. (3), we have taken into account that decrease in the group velocity near $k = 0.5$ is analogous to the electrostatic limit ($q \to 0$) for a planar metal–dielectric interface.[29]

The dispersion curves in Fig. 1(b), illustrating the two types of complex solutions for the transversely (T) polarized SPPs, differ even more than in the case of L polarization. In fact, the complex-k solution results in two SPP modes, T_1 and T_2, below the light line. The mode T_2 exhibits strong attenuation even in the absence of Ohmic losses and is, therefore, not suitable for the purpose of energy transfer.[21] Similar to the L modes, the dispersion curves T_1 and T are close to each other near the light line. As the wave number increases, the mode T_1 folds backward, and the T mode ends up at the frequency $\omega_{2T}' \approx 0.18$, which is given approximately by an expression similar to Eq. (5), with $\chi_T = [3\zeta(3) + 4(a/R)^3]/[3\zeta(3) - 2(a/R)^3]$.

The above examples indicate that the complex-ω solutions of the dispersion equations (3) and (4) exhibit a distinct band structure, and the complex-k solutions result in continuous spectra for both L and T modes.

Further difference between the two types of solutions is evident from Figs. 1(c) and 1(d), where their imaginary parts are represented in the form of SPP propagation length, L_{SPP}. For the complex-k solutions, $L_{SPP} = 1/(2k_1'')$, while for the

complex-ω solutions, $L_{SPP} = -\omega_2''/(2v_g)$, with $v_g = \partial\omega_2'/\partial k_2'$ being the group velocity. It is seen that L, T, and T_1 modes attenuate at substantially different rates, which drastically depend on SPP frequency. In accordance with the general tendency, the energy of an SPP dissipates slower near the light line, where its confinement is weak.[17] Even in this case, L modes decay within a distance that does not exceed 5 μm. The propagation length for T_1 mode is technically unlimited (when $\omega \to 0$) but is practically of the same order as for L modes, if similar localization scales are considered. Full-blown numerical simulations in the absence of gain indicate that $L_{SPP} \lesssim 1$ μm, for SPPs with spatial localization of $\sim 4R$ (regardless of the mode type).[23] Short propagation lengths of SPPs along LCMNs embedded in passive media are confirmed by recent experiments.[50]

As we stated earlier, the two types of complex solutions lead to different dispersions of SPPs, because they describe two physically distinct scenarios. From a mathematical viewpoint, these scenarios are characterized by solutions to the same system of partial differential equations with the Neumann and Dirichlet boundary conditions. The divergency of the dispersion curves, however, becomes smaller in the absence of material losses. This fact is illustrated in Fig. 1, by the dashed curves that correspond to $\gamma = 0.01$ eV. It is seen that if γ is gradually decreased, the dispersions of the complex-k and complex-ω types come closer and closer together, and overlap each other below the light line when $\gamma = 0$.[40]

It is quite instructive to analytically calculate corrections to the real wave number and real frequency in the case of small Ohmic losses. As a first example, consider the complex-k solution and the longitudinally polarized SPP mode. Let (ω_0, k_0) be the real-valued solution of Eq. (3) for $\gamma = 0$, while $(\omega_0, k_0 + k_\gamma' + ik_\gamma'')$ is the complex solution of the same equation for $\gamma \ll \omega$. Then expanding Eq. (3) in Taylor series near the point (ω_0, k_0) and assuming that $k_\gamma', k_\gamma'' \ll k_0$, we arrive at the following result:

$$k_\gamma' + ik_\gamma'' \approx -\frac{3\varepsilon_h}{2a}\frac{(a/R)^3(\omega_p/\omega_0)^2}{[\varepsilon_h - \varepsilon_\infty + (\omega_p/\omega_0)^2]^2}\frac{\gamma/\omega_0}{\Psi_2 - iq_0a\Psi_1},$$

where $q_0 = n_h\omega_0/c$ and

$$\Psi_j = \mathrm{Li}_j\{\exp[i(q_0 + k_0)a]\} - \mathrm{Li}_j\{\exp[i(q_0 - k_0)a]\}.$$

One can see that both the real and imaginary additions to the wave number scale linearly with γ. The propagation length $L_{SPP} = 1/(2k_\gamma'')$ calculated with $\gamma = 0.01$ eV is shown in Fig. 1(c) by opened circles.

Similar analysis can be readily performed for the complex-ω solution, with the result

$$\omega_\gamma' + i\omega_\gamma'' \approx -\frac{3\varepsilon_h}{2}\frac{\gamma(a/R)^3(\omega_p/\omega_0)^2}{[\varepsilon_h - \varepsilon_\infty + (\omega_p/\omega_0)^2]^2} \times \left\{(q_0a)^2\Phi_1 + i(q_0a)^3 + \frac{3\varepsilon_h(a/R)^3(\omega_p/\omega_0)^2}{[\varepsilon_h - \varepsilon_\infty + (\omega_p/\omega_0)^2]^2}\right\}^{-1},$$

and, analogously, for the transversely polarized SPP modes.

IV. DISPERSION OF SPP MODES IN THE PRESENCE OF GAIN

In order to force SPPs to travel loss-free over a distance that considerably exceeds their natural propagation length, one needs to introduce gain into the host medium. The gain Γ (which is related to the imaginary part of the refractive index via $\Gamma = -n_h''\omega/c$) not only reduces damping of the plasmon resonance in individual nanospheres, but also amplifies the radiated electromagnetic field. Due to the strong dispersion of damping, the full loss compensation over some bandwidth requires a particular frequency dependance of gain. As the gain profile is generally not of the desired form,[51] certain spectral components from the bandwidth of interest are amplified, while the rest are attenuated. Estimations show that in order to noticeably increase the propagation length of SPPs near the surface-plasmon resonance, $\Gamma \gtrsim 1500$ nm^{-1} ($n_h'' \lesssim -0.01$) is required. Gains of such magnitudes can be practically realized by either optical or electrical pumping of specially prepared active media.[35,37,52]

The effect of gain on SPP dispersion is illustrated in Fig. 2 for silver nanospheres embedded in the medium with $n_h = 1.5 - 0.02i$ (the steeply decaying mode T_2 is not shown). An important modification in the SPPs' spectra due to gain is clearly seen below the light line: The dispersion branches for L and T modes representing different complex solutions become closer to each other and overlap within broad spectral regions shaded in green. As can be seen from Figs. 2(c) and 2(d), SPP propagation in these regions occurs for larger distances than in the absence of gain ($\sim$30 μm for L mode) and are the same for different types of solutions. Matching of the propagation lengths, obtained with different methods, in the

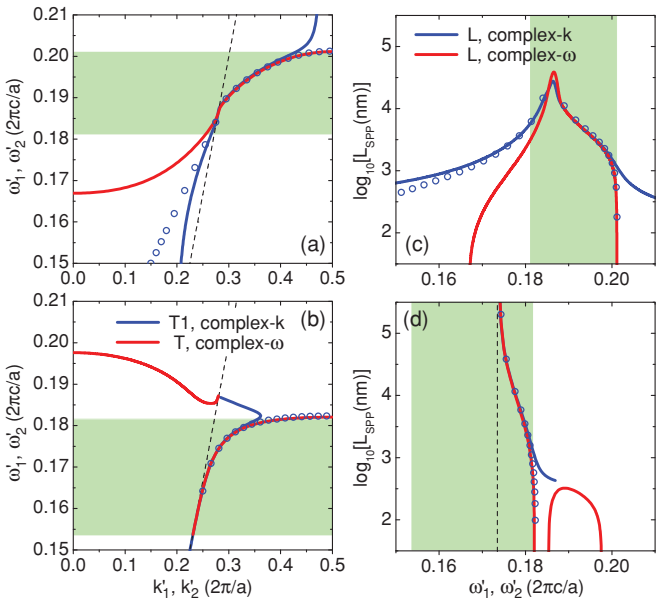

FIG. 2. (Color online) Dispersion of (a) longitudinally (L) and (b) transversely (T) polarized SPP modes for complex-k and complex-ω solutions of Eqs. (3) and (4), in the presence of gain in the host medium ($n_h'' = -0.02$); panels (c) and (d) show the corresponding propagation lengths. Shading marks the regions where the two solutions overlap; open circles show an approximate semianalytic solution given in Eqs. (7) and (8). Other parameters are the same as in Fig. 1.

low-loss regions is not a coincidence but rather a general feature of SPP dispersion.

Indeed, when attenuation of SPP modes is nearly compensated by gain, the imaginary parts of the complex-k and complex-ω solutions are small, so that we can simplify the dispersion equation $F(\omega,k) = 0$ by expanding the function F in a Taylor series and keeping only the first two terms, i.e.,

$$F(\omega_1',k_1' + ik_1'') \approx F(\omega_1',k_1') + ik_1''\frac{\partial F}{\partial k}\bigg|_{\omega_1',k_1'}, \quad (6a)$$

$$F(\omega_2' + i\omega_2'',k_2') \approx F(\omega_2',k_2') + i\omega_2''\frac{\partial F}{\partial \omega}\bigg|_{\omega_2',k_2'}. \quad (6b)$$

The dispersion curves $\omega_1'(k_1')$ and $\omega_2'(k_2')$ are close to each other in the spectral range of weak SPP damping, leading to $F(\omega_1',k_1') \approx F(\omega_2',k_2')$ and

$$v_g \approx \frac{\partial \omega_j'}{\partial k_j'} \approx -\frac{\partial F}{\partial k}\bigg/\frac{\partial F}{\partial \omega} = -\frac{\omega_2''}{k_1''}, \quad j = 1, 2,$$

where the partial derivatives of F are calculated at points $(\omega_1',k_1') \approx (\omega_2',k_2')$. This result, in turn, implies that propagation lengths corresponding to the two types of complex solutions are the same.

Thereby, we arrive at an important general conclusion that either complex-k or complex-ω solutions of the dispersion equation can be used to describe propagation of SPPs in the low-loss regime, when the Ohmic and radiation losses are almost overcome by gain. Of course, since Eq. (6) does not assume any particular form of the dispersion relation, this conclusion goes beyond SPPs in LCMNs, and is valid for an arbitrary dissipative system.[53]

Using Eq. (6a), the propagation length of SPPs can be approximated as

$$L_{\mathrm{SPP}}(k') \approx \frac{\mathrm{Im}(\partial F/\partial k)}{2\,\mathrm{Re}\,F}\bigg|_{\omega'(k'),k'}, \quad (7)$$

where the dispersion law $\omega'(k')$ is found from the real equation

$$\mathrm{Re}\left(F\frac{\partial F}{\partial k}\right) = 0, \quad (8)$$

which is obviously simpler than Eqs. (3) and (4). The approximate SPP dispersion and L_{SPP}, shown in Fig. 2 by open circles, are seen to be in good agreement with the exact dependencies shown by solid curves. Expressions analogous to Eqs. (7) and (8), and leading to the same result, can be derived starting from Eq. (6b). It should also be noted that Eq. (7) has been derived earlier in a slightly different form, by considering the problem of SPP propagation in chains of pure metallic spheroids.[40]

It is worth noting that gain has little effect on SPP dispersion obtained with the complex-ω solution [compare panels (a) and (b) in Figs. 1 and 2], but predominantly alters the dispersion of the complex-k type. For example, if $n_h'' = -0.06$, the complex-k function $\omega_1'(k_1')$ in Fig. 1(a) almost coincides with the function $\omega_2'(k_2')$ below the light line. Most importantly, the amplification threshold for L-polarized SPPs is larger than that for T-polarized SPPs. This is evident from Figs. 1(c) and 1(d), where the L-polarized modes are still subjected to damping for $n_h'' = -0.02$, while the T-polarized modes exhibit amplification below the critical frequency $\omega_c \approx 0.173$

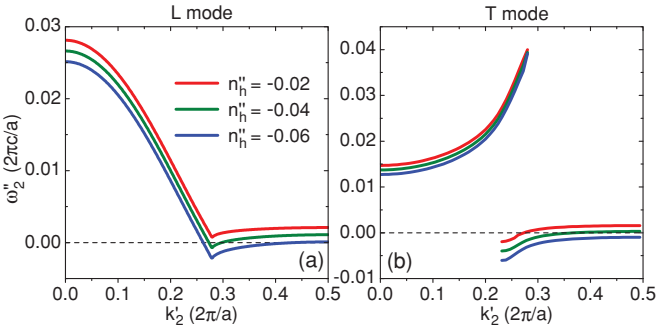

FIG. 3. (Color online) Imaginary part of complex frequency for different amounts of gain in the host medium; left and right panels correspond to L- and T-polarized SPP modes, respectively. For simulation parameters refer to text.

marked by the vertical dashed line. Figure 3 shows how the amplification bandwidth varies with gain for the complex-ω solution. It is seen that when $n_h'' = -0.04$, the T mode is amplified within a broad band $0.23 < k < 0.35$, while the L mode is only amplified in the immediate vicinity of $k \approx 0.28$. Remarkably, the dependance $\omega_2'(k_2')$ is almost the same for all curves in Fig. 3.

We also note that the complex-ω dispersion curves in Figs. 1 and 2 differ from the plots obtained for similar material parameters assuming that SPP frequency is close to the surface-plasmon resonance.[39]

V. EFFECT OF SPP DISPERSION ON PULSE PROPAGATION

As has been stated earlier, the dispersion relations and propagation lengths, obtained for SPP modes in an infinitely long LCMN, are directly applicable to realistic LCMNs consisting of a sufficiently large number of nanospheres. We study the evolution of SPP modes along a finite-length LCMN by simulating the propagation of a SPP pulse—the scenario that is often met in practice and described by the complex-k solution. Practically, a SPP can be excited by the metallic nanotip of a near-field scanning optical microscope (NSOM), which is commonly modeled by a point dipole.[50,54,55] To be consistent with the inclusion of dipolar radiation fields in our model, we consider the near-, intermediate-, and far-zone electric fields generated by the nanotip. As we shall see below, such a treatment gives considerably different results as compared to the situation when the excitation of only the first nanosphere is taken into account.[7,40]

Consider a point-dipole source placed at distance a away from the first nanosphere (along the chain axis), and suppose that the source generates electric field with the spectrum $\tilde{E}(\omega)$. Then the complex amplitude of the driving field at the position of the nth nanosphere is given by the expression

$$\tilde{E}_n^{(\mathrm{ext})} = \frac{2\tilde{E}(\omega)}{\varepsilon_h}\frac{1 - iqna}{(na)^3}\exp(iqna)$$

for the L-polarized SPP mode, and by

$$\tilde{E}_n^{(\mathrm{ext})} = -\frac{\tilde{E}(\omega)}{\varepsilon_h}\frac{1 - iqna - (qna)^2}{(na)^3}\exp(iqna)$$

for the T-polarized SPP mode.

Propagation of a SPP pulse along an LCMN is governed by the coupled-dipole equations (2), which can be written in the form

$$\mathcal{M}\,\tilde{\mathbf{p}} = \tilde{\mathbf{E}}^{(\mathrm{ext})}, \tag{9}$$

where $\mathcal{M}$ is the $N\times N$-matrix with the following elements:

$$M_{nj} = \frac{\delta_{nj}}{\alpha} - \frac{2\Delta_{nj}}{\varepsilon_h}\frac{1 - iq|n-j|a}{(|n-j|a)^3}\exp(iq|n-j|a)$$

for L polarization, and

$$M_{nj} = \delta_{nj}/\alpha + \frac{\Delta_{nj}}{\varepsilon_h}\frac{1 - iq|n-j|a - (q|n-j|a)^2}{(|n-j|a)^3}\exp(iq|n-j|a)$$

for T polarization; δ_{nj} is the Kronecker delta and $\Delta_{nj} = 1 - \delta_{nj}$ is the complementary delta. In the adopted notations, excitation of the first nanosphere is described by the field $\tilde{E}_1^{(\mathrm{ext})}$ in Eq. (9).

To illustrate the results of the previous two sections, we simulate propagation of a Gaussian pulse, $\tilde{E}(\omega) \propto \exp[-(\omega - \omega_0)^2/\Delta\omega^2]$, along a 7.5-$\mu$m-long LCMN composed of 100 silver nanospheres. We assume that the pulse is centered at frequency $\omega_0 = 0.18$ and set its bandwidth $\Delta\omega = 0.04$, which approximately corresponds to the full width at half maximum (FWHM) of 1 fs. The other parameters are the same as in Sec. III.

Figure 4 shows relative magnitudes of different dipole moments for L- and T-polarized SPPs. Specifically, solid curves in Figs. 4(a) and 4(b) show the SPP spectra for the 40th nanosphere. One can see that the L-polarized SPPs attenuate stronger than the T-polarized SPPs (regardless of whether gain is present or not), as suggested by Figs. 1(c), 1(d), 2(c), and 2(d). Since dispersion of the T_1 mode goes along the light line as frequency approaches zero, there is no low-frequency gap in the transmission spectra for T-polarized SPPs. For comparison, the dashed curves in Figs. 4(a) and 4(b) illustrate the situation where only the first nanosphere is excited by the NSOM nanotip. It is seen that such an assumption results in underestimation of the bandwidth for L and T modes, as well as overestimation of the SPPs' attenuation rates.

The density plots in Figs. 4(c)–4(f) visualize the evolution of the pulse's spectrum along the entire LCMN. In the absence of gain, the energy of L SPPs decrease by a factor of $\sim\exp(-10) \approx 5\times 10^{-5}$ at the end of the LCMN, while a similar decrease for T SPPs is only $\sim$0.01.

Three main consequences of introducing gain into the host medium are clearly seen. First, the gain opens a narrow transmission window $0.182 < \omega < 0.188$ for the L-polarized SPPs. Second, the transmission window for the T-polarized SPPs becomes wider by about $\delta\omega \approx 0.01$. Third, spectral components near the transmission band edge for T SPPs got amplified. All these features can be qualitatively predicted by analyzing SPP dispersion with Eqs. (3) and (4) or their simplified versions in Eqs. (7) and (8).

As a concluding remark, it is worth noting that the transmission windows for L and T modes have distinguished boundaries and do not overlap. The sharp separation of these windows (at $\omega \approx 0.18$ for $n_h'' = -0.02$) can be used in the design of an LCMN-based polarization filter.

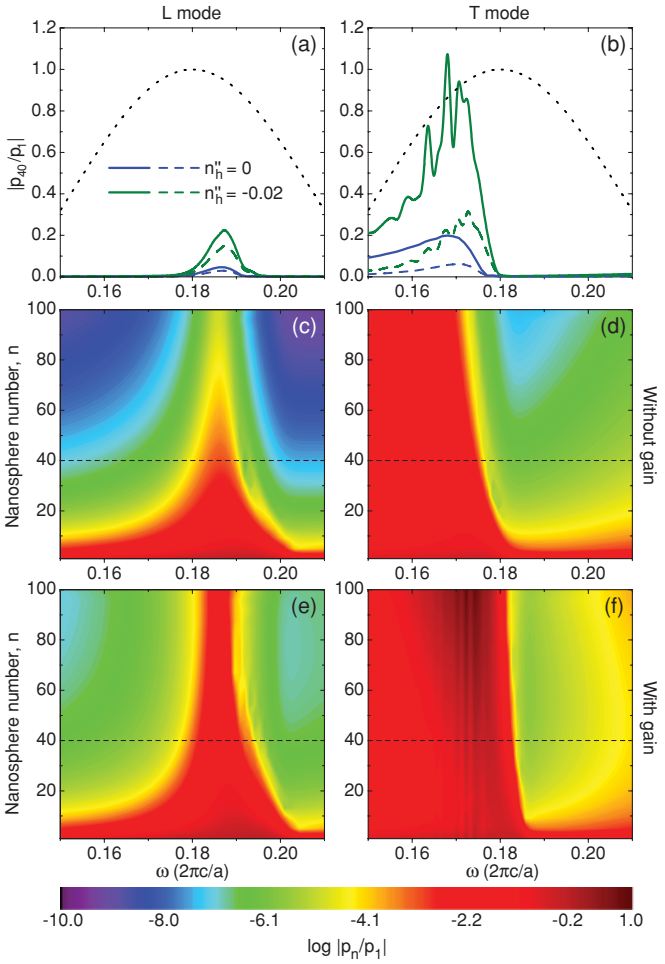

FIG. 4. (Color online) Spectra of the dipole moment modeling 40th nanosphere for (a) L-polarized and (b) T-polarized SPP pulses ($n_h'' = -0.02$); dashed curves correspond to the excitation of the first nanosphere; dotted curves show Gaussian profiles of the input pulses. Spectra of 100 dipole moments upon transmission of (c), (e) L-polarized and (d), (f) T-polarized Gaussian pulses; panels (c), (d) and (e), (f) correspond to passive and active (with $n_h'' = -0.02$) host media, respectively; dashed lines show the position of the 40th nanosphere. Other parameters are the same as in Fig. 2.

Transmitting an arbitrarily polarized SPP pulse through an LCMN, one may fully polarize the pulse in either L or T directions.

VI. CONCLUSION

In summary, we have shown that the complex-ω and complex-k solutions of the dispersion equation for the coupled dipoles lead to the same propagation characteristics of the nonradiative SPPs, when SPP damping is nearly compensated by gain in the host medium. As this takes place, the attenuation rates for SPP modes can be calculated from the simplified version of the dispersion equation; the results for the two types of complex solutions are related through the SPP's group velocity. We also demonstrated that the inclusion of gain has a strong impact on the transversely polarized SPPs, forcing them to decay on longer scales than the longitudinally

polarized ones. Together with a wide transmission window for the transversely polarized SPPs, this feature suggests them for broadband data transfer applications. Hence, LCMNs embedded in active dielectrics can serve as power-efficient, polarization-sensitive plasmonic waveguides on future, all-optical photonic chips.

ACKNOWLEDGMENTS

The work of I. D. Rukhlenko and M. Premaratne was sponsored by the Australian Research Council (ARC) through its Discovery Grant schemes under Grants No. DP0877232 and No. DP110100713.

*ivan.rukhlenko@monash.edu

[1] D. K. Gramotnev and S. I. Bozhevolnyi, Nature Photon. **4**, 83 (2010).
[2] S. A. Maier, IEEE J. Sel. Top. Quantum Electron. **12**, 1214 (2006).
[3] W. L. Barnes, A. Dereux, and T. W. Ebbesen, Nature (London) **424**, 824 (2003).
[4] S. Lal, S. Link, and N. J. Halas, Nature Photon. **1**, 641 (2007).
[5] E. Ozbay, Science **311**, 189 (2006).
[6] S. Maier and H. Atwater, J. Appl. Phys **98**, 011101 (2005).
[7] M. Quinten, A. Leitner, J. R. Krenn, and F. R. Aussenegg, Opt. Lett. **23**, 1331 (1998).
[8] P. Berini, Phys. Rev. B **61**, 10484 (2000).
[9] J. Takahara, S. Yamagishi, H. Taki, A. Morimoto, and T. Kobayashi, Opt. Lett. **22**, 475 (1997).
[10] E. Economou, Phys. Rev. **182**, 539 (1969).
[11] D. Pile, T. Ogawa, D. Gramotnev, T. Okamoto, M. Haraguchi, M. Fukui, and S. Matsuo, Appl. Phys. Lett. **87**, 061106 (2005).
[12] S. A. Maier, P. G. Kik, and H. A. Atwater, Appl. Phys. Lett. **81**, 1714 (2002).
[13] M. Conforti and M. Guasoni, J. Opt. Soc. Am. B **27**, 1576 (2010).
[14] J. A. Gordon and R. W. Ziolkowski, Opt. Express **16**, 6692 (2008).
[15] X. Cui and D. Erni, J. Opt. Soc. Am. A **25**, 1783 (2008).
[16] K. B. Crozier, E. Togan, E. Simsek, and T. Yang, Opt. Express **15**, 17482 (2007).
[17] A. F. Koenderink and A. Polman, Phys. Rev. B **74**, 033402 (2006).
[18] A. Alù and N. Engheta, Phys. Rev. B **74**, 205436 (2006).
[19] G. Gantzounis, N. Stefanou, and V. Yannopapas, J. Phys. Condens. Matter **17**, 1791 (2005).
[20] D. S. Citrin, Nano Lett. **4**, 1561 (2004).
[21] W. H. Weber and G. W. Ford, Phys. Rev. B **70**, 125429 (2004).
[22] S. Y. Park and D. Stroud, Phys. Rev. B **69**, 125418 (2004).
[23] S. Maier, M. Brongersma, P. Kik, S. Meltzer, A. Requicha, and H. Atwater, Adv. Mater. **13**, 1501 (2001).
[24] M. L. Brongersma, J. W. Hartman, and H. A. Atwater, Phys. Rev. B **62**, R16356 (2000).
[25] A. Taflove and S. C. Hagness, *Computational Electrodynamics: The Finite-Difference Time-Domain Method* (Artech House, Boston, 2005).
[26] D. S. Citrin, Nano Lett. **5**, 985 (2005).
[27] S. A. Maier, P. G. Kik, and H. A. Atwater, Phys. Rev. B **67**, 205402 (2003).
[28] A. Pannipitiya, I. D. Rukhlenko, M. Premaratne, H. T. Hattori, and G. P. Agrawal, Opt. Express **18**, 6191 (2010).
[29] S. A. Maier, *Plasmonics: Fundamentals and Applications* (Springer, Berlin, 2007).
[30] J. D. Jackson, *Classical Electrodynamics* (Wiley, New York, 1998).
[31] C. F. Bohren and D. Huffman, *Absorption and Scattering of Light by Small Particles* (Wiley, New York, 1983).
[32] A. A. Krokhin and P. Halevi, Phys. Rev. B **53**, 1205 (1996).
[33] M. A. Noginov, V. A. Podolskiy, G. Zhu, M. Mayy, M. Bahoura, J. A. Adegoke, B. A. Ritzo, and K. Reynolds, Opt. Express **16**, 1385 (2008).
[34] S. A. Maier, Opt. Commun. **258**, 295 (2006).
[35] N. M. Lawandy, Appl. Phys. Lett. **85**, 5040 (2004).
[36] A. Y. Smuk and N. M. Lawandy, Appl. Phys. B. **84**, 125 (2006).
[37] M. A. Noginov, G. Zhu, M. Bahoura, J. Adegoke, C. E. Small, B. A. Ritzo, V. P. Drachev, and V. M. Shalaev, Opt. Lett. **31**, 3022 (2006).
[38] M. A. Noginov, G. Zhu, A. M. Belgrave, R. Bakker, V. M. Shalaev, E. E. Narimanov, S. Stout, E. Herz, T. Suteewong, and U. Wiesner, Nature (London) **460**, 1110 (2009).
[39] D. S. Citrin, Opt. Lett. **31**, 98 (2006).
[40] A. A. Govyadinov and V. A. Markel, Phys. Rev. B **78**, 035403 (2008).
[41] A. Wokaun, J. P. Gordon, and P. F. Liao, Phys. Rev. Lett. **48**, 957 (1982).
[42] R. D. Averitt, S. L. Westcott, and N. J. Halas, J. Opt. Soc. Am. B **16**, 1824 (1999).
[43] L. Lewin, *Dilogarithms and Associated Functions* (McDonald, London, 1958).
[44] D. Bailey, P. Borwein, and S. Plouffe, Math. Comput. **66**, 903 (1997).
[45] C. Oubre and P. Nordlander, J. Phys. Chem. B. **109**, 10042 (2005).
[46] H. Raether, *Surface Plasmons on Smooth and Rough Surfaces and on Gratings* (Springer, Berlin, 1988).
[47] A. Burin, H. Cao, G. Schatz, and M. Ratner, J. Opt. Soc. Am. B **21**, 121 (2004).
[48] J. Pitarke, V. Silkin, E. Chulkov, and P. Echenique, Rep. Prog. Phys. **70**, 1 (2007).
[49] G. Arfken, *Mathematical Methods for Physicists* (Academic, Orlando, 1985).
[50] S. A. Maier, P. G. Kik, H. A. Atwater, S. Meltzer, E. Harel, B. E. Koel, and A. A. Requicha, Nature Mater. **2**, 229 (2003).
[51] R. Paschotta, *Encyclopedia of Laser Physics and Technology* (Wiley, New York, 2008).
[52] J. A. Gordon and R. W. Ziolkowski, Opt. Express **15**, 2622 (2007).
[53] K. C. Huang, E. Lidorikis, X. Jiang, J. D. Joannopoulos, K. A. Nelson, P. Bienstman, and S. Fan, Phys. Rev. B **69**, 195111 (2004).
[54] S. Kawata, Y. Inouye, and P. Verma, Nature Photon. **3**, 388 (2009).
[55] C. Wu, M. Ye, and H. Ye, J. Opt. A **6**, 1082 (2004).